Analyzing the impact of wind turbines on operational weather radar products

Günther Haase[1], Daniel Johnson[1] and Kjell-Åke Eriksson[2]

[1]*Swedish Meteorological and Hydrological Institute, S-60176 Norrköping, Sweden, gunther.haase@smhi.se, daniel.johnson@smhi.se*

[2]*Swedish Defence Materiel Administration, Rådhusgatan 100, Box 3021, S-83103 Östersund, Sweden, kjell-ake.eriksson@fmv.se*

Günther Haase

1. Introduction

Several studies have shown that wind farms or even single wind turbines can have a negative impact on the quality of weather radar products (Seltmann et al. 2010, Gallardo et al. 2008, Hutchinson and Miles 2008, Isom et al. 2008). Wind turbines in the vicinity of Doppler weather radars could result in clutter, beam blockage, and inaccurate Doppler velocity measurements caused by the rotating blades. This may lead to incorrect weather warnings and forecasts which itself constitutes a danger for e.g. air safety. Therefore it is very important to quantify the effect of existing wind turbines and develop strategies how to mitigate the impact of future installations.

In 2009, ca. 1400 Swedish wind turbines produced 2.5 TWh which is about 2% of the country's total power production (information from the Swedish Energy Agency). As the Swedish government promotes the expansion of wind power to 30 TWh until 2020, whereof 20 TWh will be on-shore, the number of applications for wind turbine building permits has increased considerably in the recent months. Concerning weather radars, the Swedish Armed Forces process these issues employing the OPERA guidelines (OPERA 2006), i.e. within 5 km radius from the radar applications for new wind turbines are rejected, between 5 and 20 km the possible impact is evaluated semi-automatically using a simple software tool, and beyond 20 km no restrictions exist.

Recently, the Swedish Energy Agency has funded a national research project, VINDRAD, focusing on the cohabitation between wind turbines and weather radars. Project partners are the Swedish Meteorological and Hydrological Institute, the Swedish Armed Forces, and the Swedish Defence Materiel Administration. The main objective is to develop a web-based objective decision support system to be applied by the staff issuing building permits for wind turbines and also the wind farm developers themselves. In a first stage we focus on analyzing the impact of wind turbines on operational weather radar products derived from reflectivity and wind measurements.

2. Data

2.1. Weather radars

The Swedish weather radar network consists of 12 C-band Doppler radars covering the country almost completely. Each radar measures reflectivity and radial wind with an update time of 5 minutes for the lowest elevation scan (0.5°) and 15 minutes for the other scans. Relevant radar features are summarized in Table 1 while the production chain is described in Michelson (2006).

Table 1: Selected features of the Swedish weather radars

Elevation angles	0.5°, 1.0°, 1.5°, 2.0°	2.5°, 4.0°, 8.0°, 14.0°, 24.0°, 40.0°
Measurement radius	240 km	120 km
Radial resolution	2 km	1 km
Azimuthal resolution	0.86°	0.86°
Beam width	0.9°	0.9°
PRF	600/450 Hz	1200/900 Hz

The noise threshold for reflectivities is -30 dBZ. Due to the Doppler dilemma observed radial velocity is limited to ±24 m/s for the elevation angles up to 2.0° and ±48 m/s for the remaining elevation angles.

2.2. Wind turbines

In the recent years numerous wind turbines have been built in the vicinity of the Swedish weather radars. Detailed information about all objects high enough to disturb the air traffic has been provided by the Air Navigation Services of

Sweden. The obstacle data base (ODB) contains the type of obstacle (e.g. wind turbine), the location (WGS-84 and RT90 coordinates), the height (above sea and ground level), and the Aviation Information Publications (AIP) date. Note that the AIP date represents the date when an obstacle has been modified or added to the ODB. However, wind farm developers are sometimes forced to postpone a planned wind turbine installation, i.e. the AIP date is only a vague indicator of the actual start of operation.

3. Analysis

In the analysis we focused on the lowest elevation scan (0.5°) where wind turbines penetrate the three-dimensional radar beam assuming standard propagation. It is expected that any possible impact of those turbines is most probably detectable. Considering this we limit our evaluation to turbines around Karlskrona radar (7) and Vara radar (20). Some of them are placed individually, others are grouped to smaller wind farms. However, a single radar pixel does not contain more than three wind turbines.

3.1. Clutter

The in-built Doppler filter is able to filter the static part of the wind turbine, i.e. the tower and to some extent the nacelle. However, as the blades are rotating when the wind turbine is in operation, they will not be removed and hence become visible in the radar products. The intensity of clutter highly depends on the alignment of the moving parts, i.e. the wind direction. To estimate the magnitude of clutter caused by wind turbines we decided to exclude pixels contaminated by precipitation. This can be achieved by selecting pixels which are wet (Z>-30 dBZ) in the 0.5º elevation scan and dry (Z=-30 dBZ) in the 2º elevation scan.

3.2. Beam blockage

Beam blocking effects are expected mainly behind wind turbines but they could be visible even in the adjacent azimuth gates depending on the scanning mode. A simple mean to estimate the detrimental impact of nearby wind farms is to accumulate radar precipitation over a long time interval. Due to diffraction and partial beam filling the shadowing effect diminishes at far range.

3.3. Doppler winds

Recent simulations and experiments have identified radial blade motion in the Doppler spectrum of wind turbines (Seltmann et al. 2010, US D.o.D. 2006). As mentioned before (section 3.1) the alignment of the blades relative to the radar defines the degree of disturbance. Maximum impact is expected when the rotor axis is perpendicular to the radar beam. The blade movements towards and away from the radar superpose to the final radial velocity depending on the illuminated components of the wind turbine.

4. Case study

Figure 1 shows the topography and the registered flight obstacles within a radius of 50 km around Karlskrona radar, Sweden (56.30°N, 15.61°E, 123 m a.s.l.). The Brunsmo wind farm is located approximately 13 km north-east of the radar at ca. 100 m a.s.l. Five GE wind turbines each with three blades were erected in October and November 2009, but due to problems with the power supply they were not put into operations before spring 2010. The hub height of the tower and the rotor diameter are 100 m, respectively, i.e. the rotor penetrates the radar beam completely under standard propagation conditions. Three out of five wind turbines are located at one single radar pixel (azimuth gate 52, range bin 7) which makes it very attractive to evaluate that pixel including its neighbors in more detail.

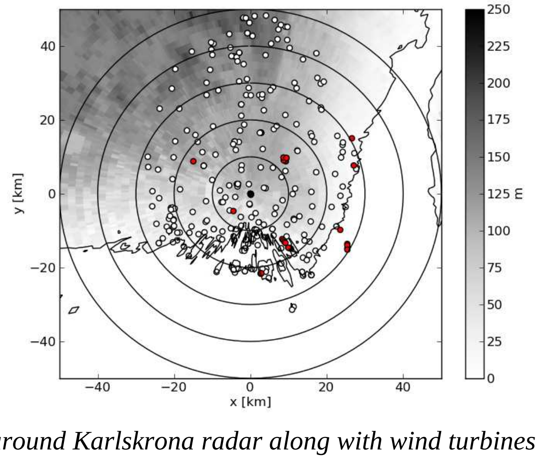

Fig 1: Topography around Karlskrona radar along with wind turbines (red dots) and other obstacles (white dots) registered on 19 January 2010. The range ring spacing is 10 km.

4.1. Clutter

The beam height (a.g.l.) at the wind turbines is 123 m for the 0.5º elevation scan and 464 m for the 2º elevation scan, respectively. That means that the radar reflectivities and winds shown in Fig 2 and 3, respectively, most likely originate from non-meteorological targets like insects, birds, vegetation, buildings etc.

As clutter inheres a seasonal dependency it is important to evaluate radar data at least one year before and (if possible) one year after a wind turbine started producing power. Still, it might be difficult to detect clutter if the signal of the obstacle is not significantly stronger than the surrounding noise. Within the analyzed time period spanning from 1 November 2008 (one year before the Brunsmo wind farm has been built) to 12 May 2010 there was a major data gap at the beginning of 2009. Generally, the clutter frequency in winter is considerably lower than in summer partly due to a less turbulent atmosphere and reduced biological activity. The most striking feature in Figs 2a-2f is the sudden rise of the noise level in March 2010 which is highly correlated with the date when the wind farm started operations. As the beam width is larger than the azimuthal resolution, the impact is even visible in the adjacent azimuth gates. Clutter beyond the wind farm is most likely caused by multiple scattered returns and also turbulence generated by the wind turbines themselves.

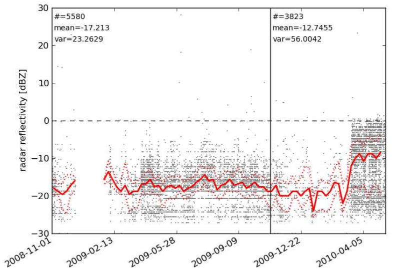

a) Azimuth gate 51, range bin 8

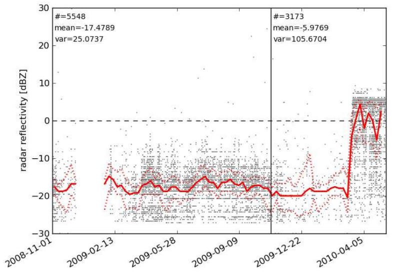

b) Azimuth gate 52, range bin 8

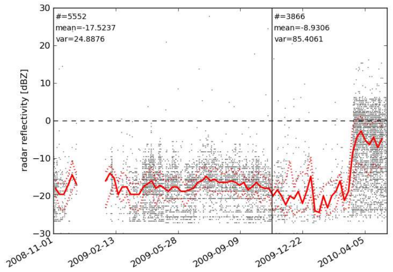

c) Azimuth gate 53, range bin 8

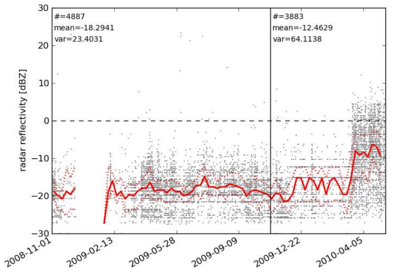

d) Azimuth gate 51, range bin 7

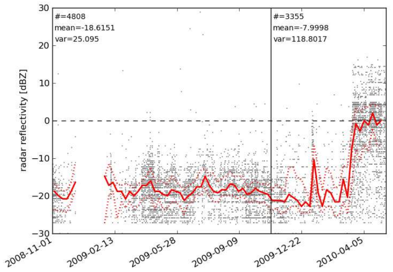

e) Azimuth gate 52, range bin 7 (WP)

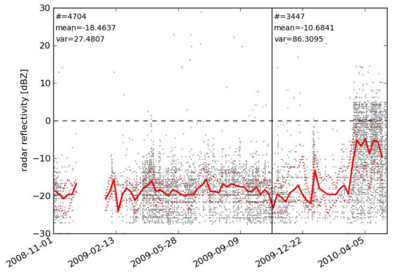

f) Azimuth gate 53, range bin 7

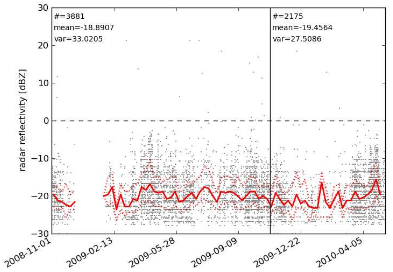

g) Azimuth gate 51, range bin 6

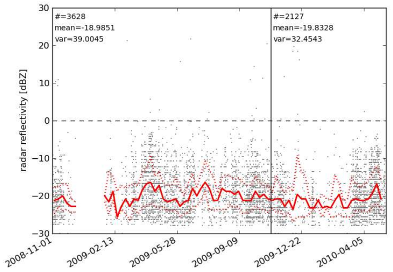

h) Azimuth gate 52, range bin 6

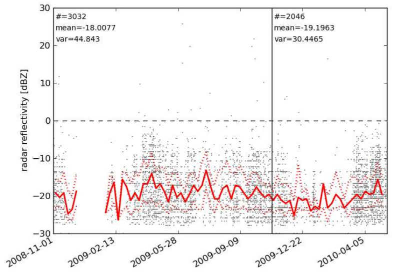

i) Azimuth gate 53, range bin 6

Fig 2: Radar reflectivities around Brunsmo wind farm (WP) for the lowest elevation scan. Note that only those pixels which are wet (Z>-30 dBZ) in the 0.5º elevation scan and dry (Z=-30 dBZ) in the 2º elevation scan are shown. The solid black line refers to the assumed date of erection. The solid red line indicates the weekly median while the dotted lines correspond to the 25th and 75th percentiles, respectively. Total number of pixels, mean and variance are calculated for each period separately.

4.2. Beam blockage

Figure 3 shows the annual precipitation relative to azimuth gate 52 (WG) derived from the lowest elevation scan before and after the Brunsmo wind farm has been built (around 1 November 2009).

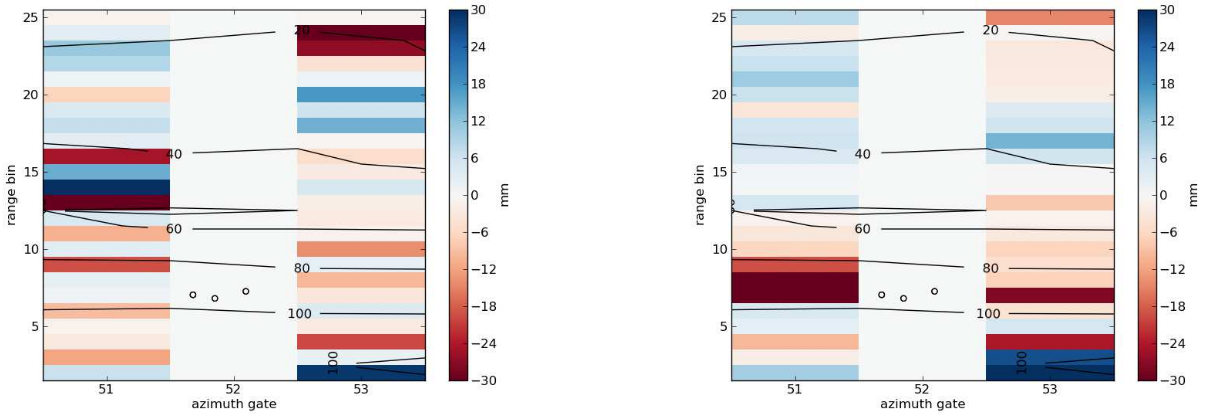

a) Before1 November 2009 *b) After1 November 2009*

Fig 3: Annual precipitation relative to azimuth gate 52 (WG) derived from the lowest elevation scan. Reddish (bluish) colors refer to pixels where the adjacent gate is drier (wetter) than WG. Contour lines represent topography [m]. The wind turbines are indicated by circles.

The local precipitation maximum at azimuth gate 53, range bin 2, is probably caused by a topographical anomaly. The reddish color at range bin 7, azimuth gates 51 and 53, indicates that WP is contaminated by clutter while the bluish color further away could be related to beam blockage effects (Fig 3b). However, the shadowing effect of the wind turbines is only minor because of the relative large distance to the radar (ca. 13 km). Moreover, even gate 51 and 53 might be affected by blockage and could not be used as a reference.

4.3. Doppler winds

The impact of wind turbines on Doppler wind measurements is illustrated in Fig 4. In the afternoon of 23 May 2010 a convective cell passed over the Brunsmo wind farm in south-easterly direction causing heavy precipitation (Figs 4a-4c). Wind turbine clutter is clearly visible in Figs 4b and 4c. The corresponding radial wind velocity fields in Figs 4d-4e reveal that most of the precipitation moves orthogonally to the radar beam (zero velocity). However, at WP the radial velocities of the hydrometeors and the blades superpose resulting in a stochastic-like behavior of velocity at that pixel.

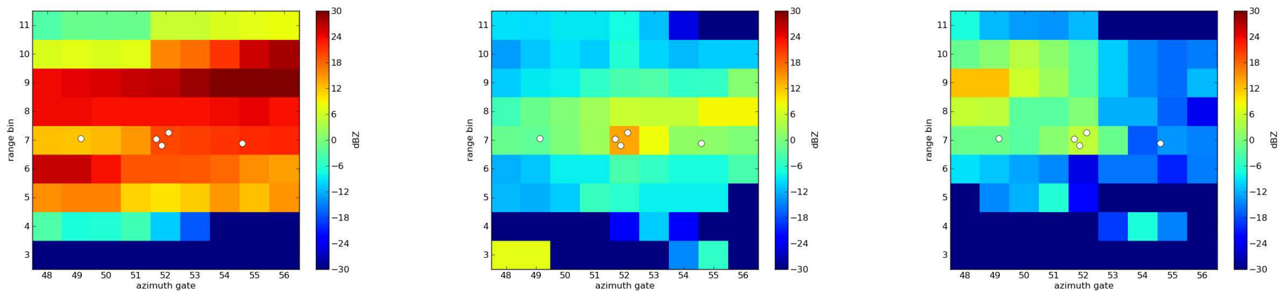

a) 23 May 2010 1530 UTC *b) 23 May 2010 1535 UTC* *c) 23 May 2010 1540 UTC*

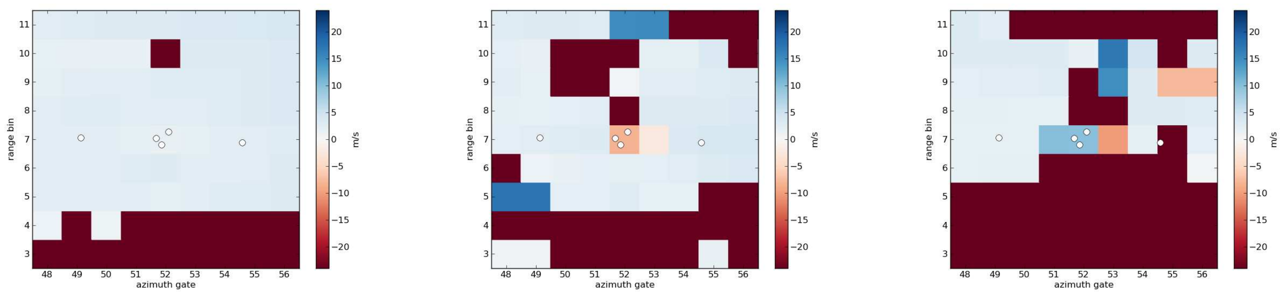

d) 23 May 2010 1530 UTC *e) 23 May 2010 1535 UTC* *f) 23 May 2010 1540 UTC*

Fig 4: Radar reflectivities (upper panel) and radial wind velocities (lower panel) around Brunsmo wind farm for the lowest elevation scan. Undetected reflectivities are colored dark blue (-30 dBZ), undetected Doppler velocities are colored dark red (-24 m/s). Wind turbines are indicated by circles.

This is confirmed by an 18-month time series of clear-air radial wind velocities at WP. The sudden rise of the reflectivity noise level (Fig 2a-2f) coincides with a significant increase of the Doppler velocity variance (Figs 5a-5f) resulting in a median velocity close to zero. As mentioned before this is probably due to the superposition of the nine blade velocities.

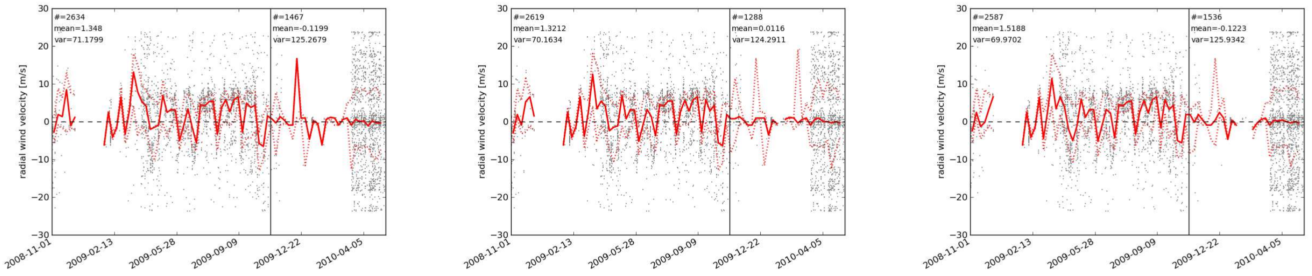

a) Azimuth gate 51, range bin 8 *b) Azimuth gate 52, range bin 8* *c) Azimuth gate 53, range bin 8*

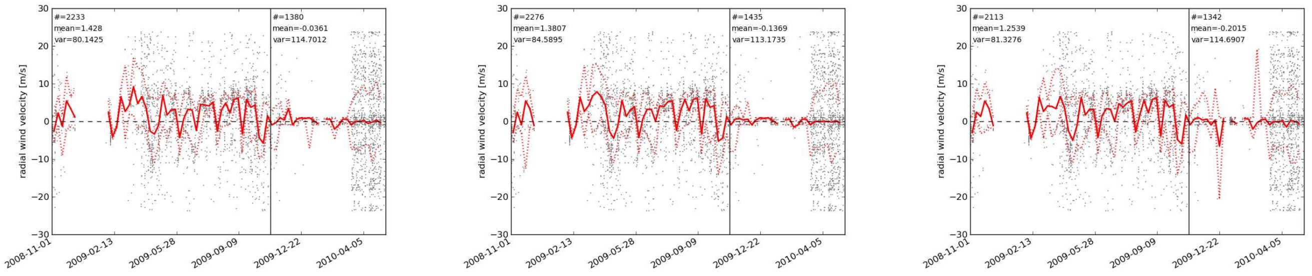

d) Azimuth gate 51, range bin 7 *e) Azimuth gate 52, range bin 7 (WP)* *f) Azimuth gate 53, range bin 7*

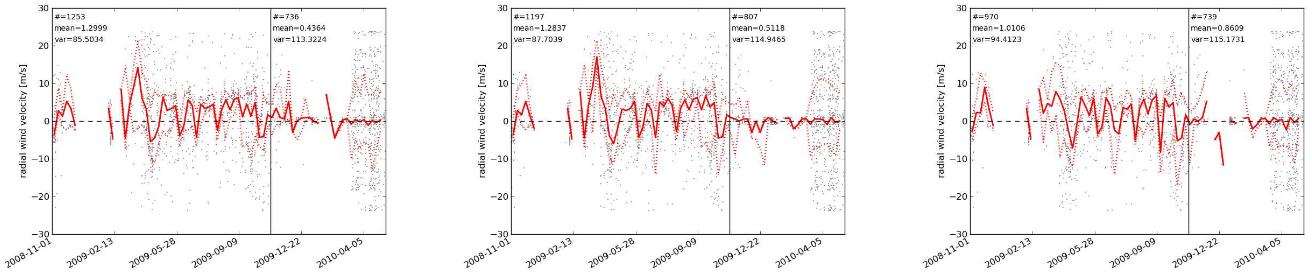

g) Azimuth gate 51, range bin 6 *h) Azimuth gate 52, range bin 6* *i) Azimuth gate 53, range bin 6*

Fig 5: As Fig 2 but for radial wind velocities.

5. Conclusions

A detailed analysis revealed an impact of wind turbines on Swedish weather radar products despite the coarse radial resolution (2 km) and a moderate sensitivity (signal-to-noise ratio). The error caused by clutter, beam blockage and inaccurate Doppler measurements has been estimated for the Brunsmo wind farm close to Karlskrona radar but the conclusions can be transferred to other wind turbines:

- Wind turbine clutter is most severe at WP, but also adjacent azimuth gates and pixels behind are contaminated.
- Beam blockage depends on the distance of the wind turbine from the radar.
- The impact of wind turbines on Doppler wind measurements is very complex, especially in case of precipitation, because the individual radial velocities of the hydrometeors and the blades superpose.

Anomalous propagation (AP) is a common phenomenon in Sweden as many radars are located close the sea. This means that the magnitude of clutter, beam blockage and erroneous Doppler winds will be even higher in case of AP because of the larger radar cross section. We have not verified this in our analysis yet but plan to do so. AP conditions could be identified using refractivity profiles derived from radiosondes or NWP models.

However, a friendly cohabitation between weather radars and wind turbines is possible. For instance, Vogt et al. (2008) formulated a proposal how to work together for mutual benefit. The VINDRAD project is another step in that direction.

Acknowledgments

The authors want to thank the Swedish Energy Agency for granting the VINDRAD project and the Air Navigation Services of Sweden for providing the flight obstacle data base.

References

Gallardo B., Pérez F., and Aguado F., 2008: Characterization Approach of Wind Turbine Clutter in the Spanish Weather Radar Network. *Proc. ERAD (2008)*.

Hutchinson, G. and Miles R., 2008: The protection of weather radar networks. The UK experience. *Proc. ERAD (2008).*

Isom B. M., Palmer R. D., Secrest G. S., Rhoton R. D., Saxion D., Allmon T. L., Reed J., Crum T., and Vogt R., 2008: Detailed Observations of Wind Turbine Clutter with Scanning Weather Radars, *J. Atmos. Oceanic Technol.*, **26**, 894-910.

Michelson D., 2006: The Swedish weather radar production chain. *Proc. ERAD (2006)*, 382-385.

OPERA, 2006: Impact of Wind Turbines on Weather Radars. WD_2006_18 available at www.knmi.nl/opera.

Seltmann J., Lang P., Stephan K., and Hengstebeck T., 2010: Impact of wind turbines on radar measurements and tracking processes. *Internal study commissioned by TI.*

US Department of Defense, 2006: The Effect of Windmill Farms On Military Readiness. *Office of the Director of Defense, Research and Engeneering*.

Vogt R. J., Crum T. D., Reed J. R., Sandifer J. B., Palmer R. D., Isom B., Snow J. T., Burgess D. W., and Paese M. S., 2008: Weather radars and wind farms - working together for mutual benefit. *Proc. WINDPOWER (2008)*.